M2 Course: Nonlinear Dynamics

Laurette TUCKERMAN

laurette@pmmh.espci.fr

Symmetry

1 Reflection Symmetry

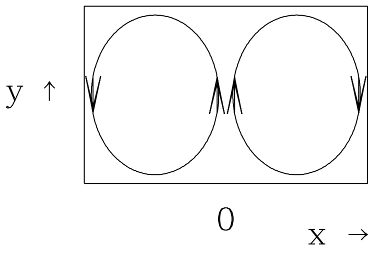

Figure 1: 2D velocity field which is symmetric under reflection in x.

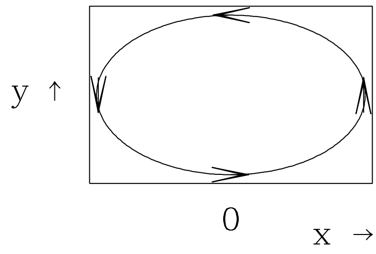

Figure 2: 2D velocity field which is antisymmetric under reflection in x.

The theory of symmetry is based on groups, the simplest of which is the two-element group $Z_2 = \{I, \kappa\}$, which describes reflection symmetry. We begin by considering a rectangular box and formalizing reflection symmetry in x for velocity fields. The velocity fields in figures 1 and 2 coincide with our intuitive picture of symmetric and antisymmetric velocity fields. The operator κ is defined to act on a 2D velocity field (u, v) via:

$$\kappa \begin{pmatrix} u \\ v \end{pmatrix} (x, y) \equiv \begin{pmatrix} -u \\ v \end{pmatrix} (-x, y) \tag{1}$$

This definition describes reflection of a vector field about the axis $x = 0$. Note that κ reverses the sign of u but not that of v, just as would a mirror. Definition (1) satisfies the essential property of a reflection operator: $\kappa^2 = I$. The symmetric velocity field of figure 1 satisfies:

$$\kappa \mathbf{u} = \mathbf{u} \tag{2a}$$

while the antisymmetric velocity field of figure 2 satisfies:

$$\kappa \mathbf{u} = -\mathbf{u} \tag{2b}$$

A general velocity field will be neither symmetric nor antisymmetric. It can be decomposed into symmetric and antisymmetric components via:

$$\mathbf{u}_s = \frac{1}{2}(I + \kappa)\mathbf{u} \tag{3a}$$

$$\mathbf{u}_a = \frac{1}{2}(I - \kappa)\mathbf{u} \tag{3b}$$

We will return to vector fields shortly, but for the moment, let us now step back and define and study some simpler reflection operators, in order to extract some important mathematical ideas. We will call each of these reflection operators by the same name, κ, although they will be different operators, acting on different kinds of objects. The operator κ and the identity I together form a *group*. A group is defined to be a set and an operation combining two elements of the set to form another element. The operation must be associative, i.e. $a(bc) = (ab)c$, but not necessarily commutative ($ab \neq ba$). There exists an identity element I, such that $aI = Ia = a$ for all a in the group, and each element a has an inverse a^{-1} such that $aa^{-1} = a^{-1}a = I$. The group $\{I, \kappa\}$ is particularly simple, since each element is its own inverse. The table describing this group is given below:

	I	κ
I	I	κ
κ	κ	I

(4)

For a function $f(x)$, we can define a reflection operator via:

$$(\kappa f)(x) \equiv f(-x) \tag{5}$$

This definition corresponds to our intuition. We have

$$(\kappa \cos)(x) = \cos(-x) = \cos(x) \Longrightarrow \kappa f = f \tag{6a}$$
$$(\kappa \sin)(x) = \sin(-x) = -\sin(x) \Longrightarrow \kappa f = -f \tag{6b}$$

Thus, $\cos(x)$ is symmetric about $x = 0$ and $\sin(x)$ is antisymmetric.

Even simpler than the function f is the scalar a, and the definition

$$\kappa a \equiv -a \tag{7}$$

Suppose a evolves according to the equation:

$$\frac{d}{dt}a = g(a) \tag{8}$$

We say that a system whose evolution is governed by g has reflection symmetry or is *equivariant* with respect to κ if

$$g\kappa = \kappa g \tag{9}$$

i.e. if g and κ commute. (Normally, one says that an equation is equivariant with respect to a group, but it is already obvious that g commutes with the identity I.) For κ defined by (7), this means that the two quantities

$$(g\kappa)(a) = g(-a) \tag{10a}$$
$$(\kappa g)(a) = -g(a) \tag{10b}$$

must be equal, i.e. that g must be an odd function of a.

Now suppose that g is a third-order polynomial, or consider the Taylor expansion of g truncated to cubic order. If g is an odd function of a, then

$$\frac{d}{dt}a = g_1 a + g_3 a^3 = (g_1 + g_3 a^2)a \tag{11}$$

which is the normal form for a pitchfork bifurcation.

Let us generalize the definition (7) to act on vectors (a, s) containing two components, one antisymmetric, a, and one symmetric, s.

$$\kappa \begin{pmatrix} a \\ s \end{pmatrix} \equiv \begin{pmatrix} -a \\ s \end{pmatrix} \tag{12}$$

(For the moment, we will use column and row vectors interchangeably.) We see that

$$\kappa \begin{pmatrix} 0 \\ s \end{pmatrix} = \begin{pmatrix} 0 \\ s \end{pmatrix} \tag{13a}$$

and

$$\kappa \begin{pmatrix} a \\ 0 \end{pmatrix} = -\begin{pmatrix} a \\ 0 \end{pmatrix} \tag{13b}$$

which coincides with definitions (2a) and (2b) of symmetric and antisymmetric vectors. We need a vector function G, which acts on and produces two-dimensional vectors, to govern the evolution of (a, s):

$$\frac{d}{dt}\begin{pmatrix} a \\ s \end{pmatrix} = G(a,s) \equiv \begin{pmatrix} g \\ h \end{pmatrix}(a,s) \tag{14}$$

G is equivariant with respect to κ of (12) if

$$\kappa \begin{pmatrix} g \\ h \end{pmatrix}(a,s) = \begin{pmatrix} g \\ h \end{pmatrix}\kappa(a,s) \tag{15}$$

i.e. if

$$\begin{pmatrix} -g \\ h \end{pmatrix}(a,s) = \begin{pmatrix} g \\ h \end{pmatrix}(-a,s) \tag{16}$$

This means that g and h must be antisymmetric and symmetric functions of a, respectively. Again specifying g and h to be third-order polynomials, or Taylor series truncated to this order, we obtain

$$\begin{aligned}
g(a,s) &= g_{00} + g_{10}a + g_{01}s + g_{20}a^2 + g_{11}as + g_{02}s^2 + g_{30}a^3 + g_{21}a^2s + g_{12}as^2 + g_{03}s^3 \\
-g(a,s) &= -g_{00} - g_{10}a - g_{01}s - g_{20}a^2 - g_{11}as - g_{02}s^2 - g_{30}a^3 - g_{21}a^2s - g_{12}as^2 - g_{03}s^3 \\
g(-a,s) &= g_{00} - g_{10}a + g_{01}s + g_{20}a^2 - g_{11}as + g_{02}s^2 - g_{30}a^3 + g_{21}a^2s - g_{12}as^2 + g_{03}s^3 \\
h(a,s) &= h_{00} + h_{10}a + h_{01}s + h_{20}a^2 + h_{11}as + h_{02}s^2 + h_{30}a^3 + h_{21}a^2s + h_{12}as^2 + h_{03}s^3 \\
h(-a,s) &= h_{00} - h_{10}a + h_{01}s + h_{20}a^2 - h_{11}as + h_{02}s^2 - h_{30}a^3 + h_{21}a^2s - h_{12}as^2 + h_{03}s^3
\end{aligned}$$

In order to satisfy (16), all terms in g containing even powers of a must vanish, while all terms in h containing odd powers of a must vanish. The result is:

$$\begin{aligned}
\begin{pmatrix} g \\ h \end{pmatrix}(a,s) &= \begin{pmatrix} g_{10}a + g_{11}as + g_{30}a^3 + g_{12}as^2 \\ h_{00} + h_{01}s + h_{20}a^2 + h_{02}s^2 + h_{21}a^2s + h_{03}s^3 \end{pmatrix} && (17) \\
&= \begin{pmatrix} (g_{10} + g_{11}s + g_{12}s^2 + g_{30}a^2)a \\ h_{00} + h_{01}s + h_{02}s^2 + h_{03}s^3 + (h_{20} + h_{21}s)a^2 \end{pmatrix} && (18) \\
&= \begin{pmatrix} \tilde{g}(a^2,s)a \\ \tilde{h}(a^2,s) \end{pmatrix} && (19) \\
&= \tilde{g}(a^2,s)\begin{pmatrix} a \\ 0 \end{pmatrix} + \tilde{h}(a^2,s)\begin{pmatrix} 0 \\ 1 \end{pmatrix} && (20)
\end{aligned}$$

The last two lines above apply to general g, h, not merely cubic polynomials. The functions $\tilde{g}$ and $\tilde{h}$ have as their arguments s and a^2, which are said to be *invariants*. An invariant f is a scalar which satisfies

$$f\kappa = f \tag{21}$$

We contrast equivariants and invariants. An equivariant is a vector function (g, h) of (a, s), as is κ, which commutes with κ. This means, in effect, that (g, h) is transformed by κ in the same way as (a, s).

$$\begin{pmatrix} -g(a,s) \\ h(a,s) \end{pmatrix} \xleftarrow{\kappa} \begin{pmatrix} g(a,s) \\ h(a,s) \end{pmatrix} \xleftarrow{G} \begin{pmatrix} a \\ s \end{pmatrix} \tag{22a}$$

$$\begin{pmatrix} g(-a,s) \\ h(-a,s) \end{pmatrix} \xleftarrow{G} \begin{pmatrix} -a \\ s \end{pmatrix} \xleftarrow{\kappa} \begin{pmatrix} a \\ s \end{pmatrix} \tag{22b}$$

i.e. $g(-a,s) = -g(a,s)$ and $h(-a,s) = h(a,s)$ as we have seen, meaning that g must be an odd and h an even function of a. An invariant is a scalar function of (a,s) which remains the same when its arguments are acted on by κ.

$$f(-a,s) \stackrel{f}{\leftarrow} \begin{pmatrix} -a \\ s \end{pmatrix} \stackrel{\kappa}{\leftarrow} \begin{pmatrix} a \\ s \end{pmatrix} \tag{23}$$

$$f(a,s) \stackrel{f}{\leftarrow} \begin{pmatrix} a \\ s \end{pmatrix} \tag{24}$$

i.e. $f(-a,s) = f(a,s)$, meaning that f must be an even function of a. The functions $f(a,s) = a^2$ and $f(a,s) = s$ both have this property, so they are both invariants. In fact, all invariants can be written as functions of a^2 and s. Expression (20) states that the most general equivariant is expressible as a superposition of a few basic equivariants (here, $(a,0)$ and (0,1)) with coefficients which are general functions of a few basic invariants (here, a^2 and s). This remains true in more complicated situations, as we will discuss later.

We emphasize the difference between a system G which is equivariant with respect to κ and a solution vector which is κ-symmetric. It is certainly not true that solutions to κ-equivariant systems are symmetric. Symmetric solutions are of the form $(0,s)$, antisymmetric solutions of the form $(a,0)$, and asymmetric solutions (neither symmetric nor antisymmetric) are of the form (a,s).

The consequence of the symmetry of G is rather this:

If (a,s) is a time-dependent or stationary solution to a κ-equivariant system (14), then $\kappa(a,s) = (-a,s)$ is also a solution.

(This follows from applying κ to both sides of (14) and commuting κ with d/dt and with G.) This statement means that asymmetric solutions (a,s), $a \neq 0$, occur in pairs $(\pm a, s)$. For example, the existence of the solution in figure 2 in a reflection-symmetric domain implies the existence of another solution, with the arrows reversed. For symmetric solutions $(0,s)$, the statement does not lead to any new solutions. This is what must happen if the solutions to G are known to be unique, for example if G is a linear system or for the Navier-Stokes equations at sufficiently low Reynolds number:

If the κ-equivariant system (14) has a unique solution, then that solution is symmetric.

Let us discuss the consequences of symmetry on a linear system, where G consists of a matrix acting on (a,s). Selecting only linear terms from (17), we get

$$\frac{d}{dt}\begin{pmatrix} a \\ s \end{pmatrix} = G\begin{pmatrix} a \\ s \end{pmatrix} = \begin{pmatrix} g_{10} & 0 \\ 0 & h_{01} \end{pmatrix}\begin{pmatrix} a \\ s \end{pmatrix} \tag{25}$$

The matrix G is diagonal, a consequence of its κ-symmetry. Thus a and s are not coupled by the linear evolution. Eigenvectors of G are either symmetric or antisymmetric, and not a superposition of the two. This will remain true in more general settings. Consider a general matrix or linear operator G, multiplication by which commutes with any reflection operator κ on a general vector or function u. Suppose now that (λ, u) is an eigenpair of G, i.e. λ is an eigenvalue of G and u the corresponding eigenvector. We have:

$$\begin{aligned} Gu &= \lambda u \\ \kappa G u &= \kappa \lambda u \\ G\kappa u &= \lambda \kappa u \end{aligned} \tag{26}$$

That is, κu is also an eigenvector of G with the same eigenvalue. There are two ways in which this may happen. One way is for κu to be a multiple of u. In this case,

$$\begin{aligned} \kappa u &= cu \\ \kappa^2 u &= \kappa c u \\ u &= c^2 u \\ c &= \pm 1 \end{aligned} \tag{27}$$

recalling that the defining property of a reflection operator is that κ^2 is the identity. Either $c = 1$, in which case u is symmetric, or $c = -1$, in which case u is antisymmetric.

Now suppose that κu is not a multiple of u. Then λ is an eigenvalue of G with two different linearly independent eigenvectors, i.e. λ is a multiple eigenvalue of G. This may happen, but is unlikely, unless parameters are especially adjusted to make it so or the system has some other special feature that we have not taken into account. For example, in (25), we would require $g_{10} = h_{01}$. This is unlikely, since symmetric and antisymmetric vectors, such as the velocity fields depicted in figures 1 and 2, would not be expected to evolve in the same way. But even if u and κu are two linearly independent eigenvectors of G, we may consider instead the pair

$$\frac{I+\kappa}{2} u \text{ which is symmetric since } \kappa \frac{I+\kappa}{2} u = \frac{\kappa + I}{2} \tag{28a}$$

$$\frac{I-\kappa}{2} u \text{ which is antisymmetric since } \kappa \frac{I-\kappa}{2} u = \frac{\kappa - I}{2} \tag{28b}$$

$$\tag{28c}$$

Let us return to the reflection operator (1) defined for 2D velocity fields and apply it to the Navier-Stokes equations:

$$\partial_t \begin{pmatrix} u \\ v \end{pmatrix} = (NS) \begin{pmatrix} u \\ v \end{pmatrix} \begin{pmatrix} NS_u \\ NS_v \end{pmatrix} \equiv \begin{pmatrix} -(u\partial_x + v\partial_y)u - \partial_x p + \nu(\partial_x^2 + \partial_y^2)u \\ -(u\partial_x + v\partial_y)v - \partial_y p + \nu(\partial_x^2 + \partial_y^2)v \end{pmatrix} \tag{29}$$

subject to

$$\partial_x u + \partial_y v = 0 \tag{30}$$

We wish to verify whether this system of equations is equivariant with respect to κ. The non-trivial part of this calculation is how to treat differentiation. We first establish that the action of differentiation on $(\kappa f)(x) \equiv f(-x)$ is $(\kappa f)'(x) = -f'(-x)$. This can be seen in various ways. Let $\tilde{f}(x) \equiv (\kappa f)(x) \equiv f(-x)$. Then:

$$\begin{aligned} \tilde{f}'(x) &\equiv \lim_{\Delta x \to 0} \frac{\tilde{f}(x+\Delta x) - \tilde{f}(x)}{\Delta x} = \lim_{\Delta x \to 0} \frac{f(-x-\Delta x) - f(-x)}{\Delta x} \\ &= \lim_{\Delta x \to 0} \frac{f(-x+\Delta x) - f(-x)}{-\Delta x} = -f'(-x) \end{aligned} \tag{31}$$

The second derivative satisfies $(\kappa f)''(x) = f''(-x)$.

Armed with these results, we calculate the action of the Navier-Stokes evolution operator NS defined in (29) on $[\kappa(u,v)]\,(x,y) \equiv (-u,v)(-x,y)$. Operation by κ is equivalent to $u, x, \partial_x \to -u, -x, \partial_x$ and $p, v, y, \partial_y \to p, v, y, \partial_y$.

$$\left[(NS)\kappa \begin{pmatrix} u \\ v \end{pmatrix}\right](x,y) = \begin{pmatrix} -((-u)(-\partial_x) + v\partial_y)(-u) - (-\partial_x)p + \nu(\partial_x^2 + \partial_y^2)(-u) \\ -((-u)(-\partial_x) + v\partial_y)v - \partial_y p + \nu(\partial_x^2 + \partial_y^2)v \end{pmatrix}(-x,y) \tag{32}$$

Acting in the opposite order, we obtain:

$$
\begin{aligned}
\left[\kappa(NS)\begin{pmatrix} u \\ v \end{pmatrix}\right](x,y) &= \begin{pmatrix} -NS_u \\ NS_v \end{pmatrix}(-x,y) \\
&= \begin{pmatrix} -[-(u\partial_x + v\partial_y)u - \partial_x p + \nu(\partial_x^2 + \partial_y^2)u] \\ -(u\partial_x + v\partial_y)v - \partial_y p + \nu(\partial_x^2 + \partial_y^2)v \end{pmatrix}(-x,y) \qquad (33)
\end{aligned}
$$

which is identical to the previous result. That the 2D Navier-Stokes equations are equivariant with respect to reflection in x is not surprising: we do not expect any general equations of continuum physics to distinguish between the left and right halves of a domain or between left-going and right-going motion.

It is boundary conditions and body forces that determine whether a system has reflection symmetry. Figures 1 and 2 depict a rectangular box. In a geometry which lacked reflection symmetry in x, there would be no possibility of reflection symmetry for the system. Even in a rectangular box, however, only certain boundary conditions will meet the requirement of reflection symmetry. General Dirichlet boundary conditions for a rectangular geometry are:

$$
\begin{aligned}
u(x = \pm 1, y) &= a_\pm(y) \\
v(x = \pm 1, y) &= b_\pm(y) \\
u(x, y = \pm h) &= c_\pm(x) \\
v(x, y = \pm h) &= d_\pm(x) \qquad (34)
\end{aligned}
$$

Acting with κ on these boundary conditions transforms the left-hand-side concerning (u, v), but not the right-hand-side concerning known functions.

$$
\begin{aligned}
-u(x = \mp 1, y) = a_\pm(y) &\implies u(x = \pm 1, y) = -a_\mp(y) \\
v(x = \mp 1, y) = b_\pm(y) &\implies v(x = \pm 1, y) = b_\mp(y) \\
-u(-x, y = \pm h) = c_\pm(x) &\implies u(x, y = \pm h) = -c_\pm(-x) \\
v(-x, y = \pm h) = d_\pm(x) &\implies v(x, y = \pm h) = d_\pm(-x) \qquad (35)
\end{aligned}
$$

The four transformed boundary conditions in (35) are equivalent to the boundary conditions (34) of the original system if

$$
\begin{aligned}
a_\pm(y) &= -a_\mp(y) \\
b_\pm(y) &= b_\mp(y) \\
c_\pm(x) &= -c_\pm(-x) \\
d_\pm(x) &= d_\pm(-x) \qquad (36)
\end{aligned}
$$

the situation depicted in figure 3.

Other types of boundary conditions, for example Neumann conditions on the normal derivatives, or a combination of Dirichlet and Neumann conditions, could also be considered. For the system to be reflection-symmetric in x, however, the boundary conditions on the left side $x = -1$ and on the right side $x = +1$ must be of the same type.

We return to the types of flows shown in figure 1 and 2 in the beginning of this section. Figure 4 shows an *asymmetric* flow $\mathbf{u}_s + \mathbf{u}_a$ (neither symmetric nor antisymmetric) and a symmetric flow. Reflection in x transforms $\mathbf{u}_s + \mathbf{u}_a$ into a different asymmetric flow $\mathbf{u}_s - \mathbf{u}_a$. Assuming reflection symmetry in x, these two flows are dynamically equivalent: it makes no difference whether fluid descends on the left and rises on the right or vice versa. Transition from a symmetric flow $\mathbf{u}_s$ to the asymmetric flows $\mathbf{u}_s \pm \mathbf{u}_a$ will

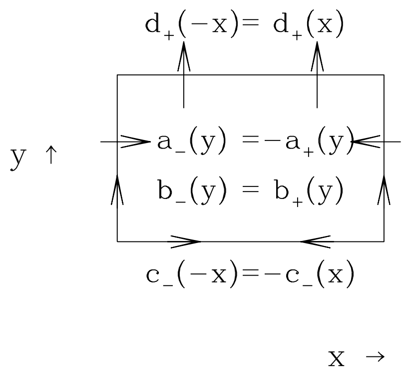

Figure 3: Boundary conditions for the 2D Navier-Stokes equations which respect x-reflection symmetry.

always occur via a pitchfork bifurcation, shown on the left in figure 5. This reasoning applies whenever the number of cells is odd.

In contrast, the symmetric flow $\mathbf{u}_s$ is unchanged under κ, as is shown in the first two columns of figure 4. The flow $-\mathbf{u}_s$ is also shown as the third column of figure 4. However, $-\mathbf{u}_s$ is in general *not* dynamically equivalent to $\mathbf{u}_s$. In $\mathbf{u}_s$, fluid descends along the walls and rises in the middle, and vice versa for $-\mathbf{u}_s$, which are in general *not* equivalent situations, unless additional conditions hold. The symmetric flow $\mathbf{u}_s$ will then be associated with a transcritical bifurcation, as shown in figure 5, where $\mathbf{u}_s$ and $-\mathbf{u}_s$ both appear, but with different properties. This reasoning applies whenever the number of cells is even and whenever the domain is bounded by lateral walls. (Periodic domains will be the subject of the next section.) For non-Boussinesq convection, or in the formation of Taylor vortices, for example, the transition to an even number of cells is via a transcritical bifurcation if the domain is of finite length. In Boussinesq convection, however, fluid rising and falling *are* equivalent, and so transition to $\pm\mathbf{u}_s$ takes place via a pitchfork bifurcation, independent of whether the number of cells is even or odd.

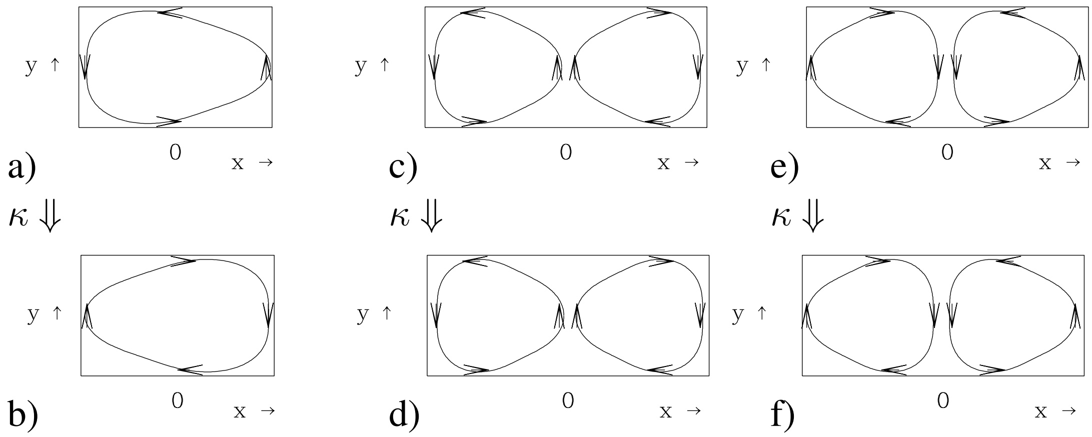

Figure 4: Left column: a) asymmetric flow $\mathbf{u}_s + \mathbf{u}_a$ is mapped into flow below (b) by the x-reflection operator κ. The two flows are therefore dynamically equivalent. Middle column: c) symmetric flow $\mathbf{u}_s$ is mapped into itself (d) by κ. Third column: e) the symmetric flow $\mathbf{u}'_s$ does not result from a symmetry operation on $\mathbf{u}_s$ and so is in general not dynamically equivalent to it.

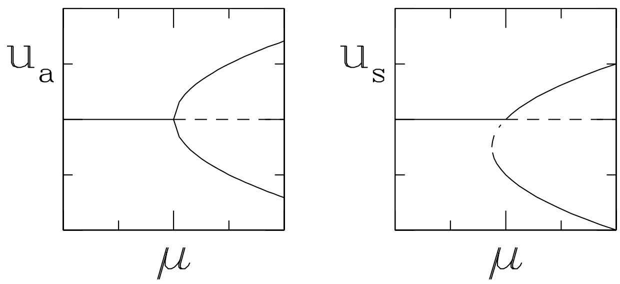

Figure 5: Pitchfork bifurcation (left) associated with bifurcation to asymmetric flow and transcritical bifurcation (right) associated to symmetric flow.

2 Rotation

2.1 Symmetry groups

The most important symmetry groups of the plane are given in Table 1.

Z_2	Z_3	Z_4	$\dots$	$SO(2)$
D_2	D_3	D_4	$\dots$	$O(2)$

Table 1: Some symmetry groups of the plane.

Z_n represents the group of rotations of an n-gon. D_n is this group with the addition of reflections about any of the axes of the n-gon. Figure 6 illustrates several of these symmetry groups. The triangle, square, and circle on the second row have symmetries D_3, D_4, and $O(2)$. In the first row, distinguishing features have been added to each of the shapes in order to break reflection symmetry. As a result, the objects on the first row have symmetries Z_3, Z_4, and $SO(2)$.

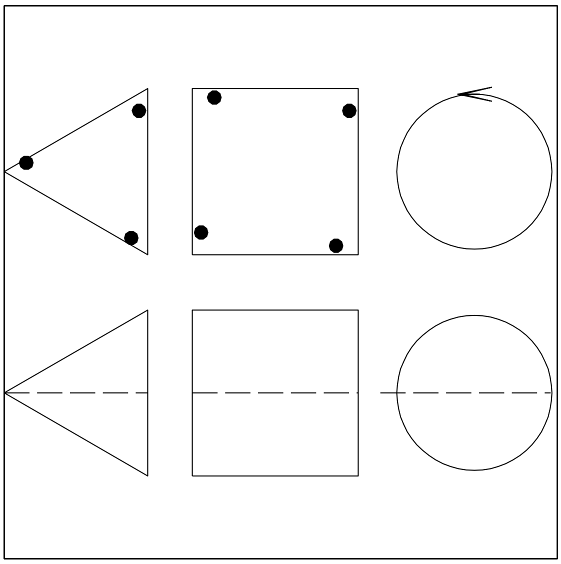

Figure 6: Objects on the first row have symmetries Z_3, Z_4, and $SO(2)$. Those on the second row have symmetries D_3, D_4, and $O(2)$.

Let us focus on $O(2)$. We begin by studying steady bifurcations. For this purpose, we represent a point (x, y) on the plane by the complex number z. We then can represent the action of rotation by θ and reflection in y by:

$$S_\theta z \equiv e^{i\theta} z \tag{37a}$$

$$\kappa z \equiv \bar{z} \tag{37b}$$

Rotation and reflection do not commute:

$$\kappa S_\theta z = \quad \kappa(e^{i\theta} z) \quad = e^{-i\theta}\bar{z} \tag{38a}$$
$$S_\theta \kappa z = \quad S_\theta \bar{z} \quad = e^{i\theta}\bar{z} \tag{38b}$$

Equations (38) show that:

$$\kappa S_\theta z = S_{-\theta}\kappa z \tag{39}$$

In fact, one reflection suffices; any reflection can be written as a combination of κ with a rotation. For example, reflection about the y axis, instead of the x axis, is $\kappa_y(x+iy) = -x+iy$.

$$\begin{aligned} -x+iy &= -(x-iy) \\ \kappa_y &= S_\pi \kappa \end{aligned} \tag{40}$$

(It is also true that $\kappa_y = \kappa S_\pi$. Exceptionally S_π is the only rotation to commute with κ, since $e^{i\theta} = e^{-i\theta}$.) S_θ and κ are called the *generators* of the group $O(2)$, since any element of $O(2)$ can be formed as combinations of these elements.

Before continuing, let us illustrate how the representation (37) acts on a function $w(\rho,\theta)$, where θ is a direction with reflection and translation symmetry. If the θ-dependence is trigonometric with azimuthal wavelength 2π, then w can be written as:

$$w(\rho,\theta,t) = \frac{1}{2}(z(\rho,t)e^{i\theta} + \bar{z}(\rho,t)e^{-i\theta}) \tag{41}$$

The real part of z can be seen as the coefficient of $\cos(\theta)$, while the imaginary part of z is the coefficient of $\sin(\theta)$. The operations (37) on z then correspond to the following operations on w:

$$(S_{\theta_0} w)(\rho,\theta) \equiv w(\rho,\theta+\theta_0) \tag{42a}$$
$$(\kappa w)(\rho,\theta) \equiv w(\rho,-\theta) \tag{42b}$$

The analysis we are undertaking describes the formation of a spatial structure in a domain normalized to the wavelength of the structure.

2.2 Circle pitchfork bifurcation

Let us now return to the abstract setting and determine which functional forms are equivariant under (37). We consider monomials of x and y or, more conveniently, of z and $\bar{z}$.

$$f(z,\bar{z}) = f_{mn} z^m \bar{z}^n \tag{43}$$

where f is complex. We have

$$\kappa f(z,\bar{z}) = \overline{f(z,\bar{z})} = \bar{f}_{mn}\bar{z}^m z^n \tag{44a}$$
$$f(\kappa(z,\bar{z})) = f_{mn}\bar{z}^m z^n \tag{44b}$$

Thus, for f to commute with κ, the coefficient f_{mn} must be real. In order for f to commute with S_θ for all θ, we calculate

$$S_\theta f(z,\bar{z}) = e^{i\theta} f(z,\bar{z}) = e^{i\theta} f_{mn} z^m \bar{z}^n \tag{45a}$$
$$f(S_\theta(z,\bar{z})) = f_{mn}(e^{i\theta}z)^m \overline{(e^{i\theta}z)}^n = f_{mn} e^{im\theta} z^m e^{-in\theta}\bar{z}^n \tag{45b}$$

Thus we require that $e^{i\theta(m-n)} = e^{i\theta}$. The only way that this can be true for all θ is for $m - n = 1$. leading to polynomials of the form:

$$\begin{aligned} f(z,\bar{z}) &= f_{10}z + f_{21}z^2\bar{z} + f_{32}z^3\bar{z}^2 + \cdots \\ &= (f_{10} + f_{21}|z|^2 + f_{32}|z|^4 + \cdots)z \\ &= \tilde{f}(|z|^2)z \end{aligned} \tag{46}$$

where $\tilde{f}$ is a general real function of $|z|^2$. In the terms introduced in the previous section, the scalar $|z|^2$ is *invariant* under the group $O(2)$ and the complex number (or two-dimensional vector) z is *equivariant*.

Truncating (46) at cubic order, we derive the evolution equation:

$$\frac{dz}{dt} = (\mu - \alpha|z|^2)z \tag{47}$$

The steady states of (47) are $z = 0$ and $|z| = \sqrt{\mu/\alpha}$, which exists only for $\mu/\alpha > 0$, as illustrated in figure 7. We consider μ to be the bifurcation parameter, such as a relative Reynolds number $(Re - Re_c)/Re_c$ or Rayleigh number $(Ra - Ra_c)/Ra_c$. The transition occurring at $\mu = 0$ is called a circle pitchfork, because a "circle" of steady states, $z = \sqrt{\mu/\alpha}\, e^{i\theta}$, is created as μ crosses zero.

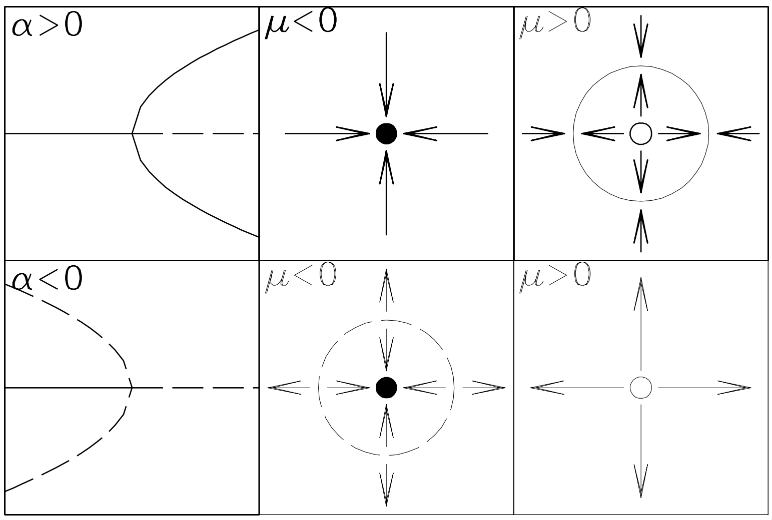

Figure 7: Circle pitchfork bifurcation. The upper diagrams correspond to the supercritical case, the lower diagrams to the subcritical case. Leftmost are the bifurcation diagrams in the (μ, r) plane, middle and rightmost are phase portraits in the (x, y) plane. Stable steady states are designated by solid dots or the solid curve. Unstable steady states are shown as hollow dots or the dashed curve.

We may write (47) in Cartesian coordinates $z = x + iy$:

$$\frac{dx}{dt} = (\mu - \alpha(x^2 + y^2))x \tag{48a}$$

$$\frac{dy}{dt} = (\mu - \alpha(x^2 + y^2))y \tag{48b}$$

or in polar coordinates $z = re^{i\theta}$:

$$\frac{d\left(re^{i\theta}\right)}{dt} = \left(\frac{dr}{dt} + ri\frac{d\theta}{dt}\right)e^{i\theta} = \left(\mu - \alpha r^2\right) r\, e^{i\theta} \tag{49}$$

$$\frac{dr}{dt} = (\mu - \alpha r^2)\, r \tag{50a}$$

$$\frac{d\theta}{dt} = 0 \tag{50b}$$

Equation (50a) shows that the amplitude r undergoes an ordinary pitchfork bifurcation and (50b) shows that the phase θ shows no tendency to move. The stability of the trivial state and the bifurcating circle of states can be calculated from either (48) or (50) via the Jacobian matrix:

$$J(x,y) = \begin{pmatrix} \mu - \alpha(3x^2+y^2) & -2\alpha xy \\ -2\alpha xy & \mu - \alpha(x^2+3y^2) \end{pmatrix} \tag{51}$$

$$J(r,\theta) = \begin{pmatrix} \mu - \alpha 3r^2 & 0 \\ 0 & 0 \end{pmatrix} \tag{52}$$

To calculate the stability of the trivial state, we use

$$J(x=0, y=0) = \begin{pmatrix} \mu & 0 \\ 0 & \mu \end{pmatrix} \tag{53}$$

which has μ as a double eigenvalue. The trivial state (0,0) is stable for $\mu < 0$ and has two unstable directions (corresponding to the two directions of the plane) for $\mu > 0$. Note that the polar form $J(r,\theta)$ of equation (52) would seem to indicate that the two eigenvalues of (0,0) are μ and 0. This contradictory result arises from the fact that θ is not well defined at $r = 0$, so that $J(r,\theta)$ is also not well defined at $r = 0$.

For the bifurcating circle of states, we may write

$$J(r = \sqrt{\mu/\alpha}, \theta) = \begin{pmatrix} \mu - 3\mu & 0 \\ 0 & 0 \end{pmatrix} = \begin{pmatrix} -2\mu & 0 \\ 0 & 0 \end{pmatrix} \tag{54}$$

whose eigenvalues are -2μ and 0. The circle pitchfork can be supercritical or subcritical, according to the sign of α. If $\alpha > 0$, then the circle of bifurcating states exists for $\mu > 0$ and the eigenvalue -2μ corresponds to contraction onto the circle $\sqrt{\mu/\alpha}$, i.e. stability. If $\alpha < 0$, then the circle of bifurcating states exists for $\mu < 0$ and the eigenvalue -2μ corresponds to expansion away from the circle, i.e. instability. The eigenvalue 0 corresponds to the phase invariance, i.e. the fact that the system shows no tendency to move in the direction θ. The eigenvalues can be confirmed by evaluating $J(x,y)$ of equation (51) for $x^2 + y^2 = r^2 = \mu\alpha$:

$$J(x,y) = \begin{pmatrix} -2\alpha x^2 & -2\alpha xy \\ -2\alpha xy & -2\alpha y^2 \end{pmatrix} \tag{55}$$

whose eigenvalues are:

$$-\alpha(x^2+y^2) \pm \sqrt{(\alpha(x^2-y^2))^2 + 4\alpha x^2 y^2} = \alpha(x^2+y^2) \pm \sqrt{\alpha(x^2+y^2))^2} = -\mu \pm \mu \tag{56}$$

The eigenvector corresponding to eigenvalue $\mu = 0$ resulting from phase invariance, called the *marginal* direction, points in the θ direction, i.e. it is $(0,1)$ in the polar representation and $(-y, x)$ in the Cartesian representation. Returning to functions of (ρ,θ), if $W(\rho,\theta)$ is a steady state resulting from a circle pitchfork, then W is even in θ about some point θ_0. The marginal eigenvector is $\partial W/\partial\theta$. This can be seen as follows. The dynamical system governing w is

$$\frac{dw}{dt} = \mathcal{F}(w) \tag{57}$$

where $\mathcal{F}$ is a general operator that may include differentiation in θ and/or ρ as well as other operations on the function w. The $O(2)$ symmetry implies, however, that $\mathcal{F}$ is *homogeneous* in θ, meaning that it does not distinguish between different values of θ. Since W is a fixed point, or rather, a member of a circle of fixed points,

$$0 = \mathcal{F}(W) \tag{58}$$

Differentiating equation (58) with respect to θ, we obtain:

$$0 = \frac{d\mathcal{F}(W)}{d\theta} = \frac{\delta\mathcal{F}}{\delta W}\frac{\partial W}{\partial\theta} \tag{59}$$

$\delta\mathcal{F}/\delta W$ is the Jacobian of $\mathcal{F}$, sometimes called the *Fréchet derivative* in this continuous functional context. Equation (59) shows that $\partial W/\partial\theta$ is a marginal eigenvector of $\delta\mathcal{F}/\delta W$. Note that if the operator $\mathcal{F}$ contained θ-dependent terms, then equation (59) would contain other terms resulting from differentiating $\mathcal{F}$ with respect to θ and so $\partial W/\partial\theta$ would not be an eigenvector of $\delta\mathcal{F}/\delta W$.

2.3 Drift pitchfork

After a circle of steady states has been formed, a *drift pitchfork* may occur. A set of equations showing the drift pitchfork is

$$\frac{dr}{dt} = (\mu - r^2)r \tag{60a}$$
$$\frac{d\theta}{dt} = \zeta \tag{60b}$$
$$\frac{d\zeta}{dt} = (r^2 - 1 - \zeta^2)\zeta \tag{60c}$$

The behavior of equations (60) is illustrated in figure 8. For $\mu < 0$, the only solution is the origin, with $r = \zeta = 0$. Equation (60a) shows that r undergoes a pitchfork bifurcation at $\mu = \mu_{cp} = 0$, leading to a circle of steady solutions

$$r = \sqrt{\mu} \tag{61a}$$
$$\theta = \theta_0 \tag{61b}$$
$$\zeta = 0 \tag{61c}$$

Equation (60c) shows that ζ undergoes a pitchfork bifurcation at $\mu = \mu_{dp} = 1$, when $r^2 - 1 = \mu - 1 = 0$, leading to solutions:

$$r = \sqrt{\mu} \tag{62a}$$
$$\theta = \theta_0 + \zeta t \tag{62b}$$
$$\zeta = \pm\sqrt{\mu - 1} \tag{62c}$$

The velocity of θ can be either in the clockwise ($\zeta < 0$) or counterclockwise ($\zeta > 0$) direction. It is zero at onset of the motion and increases like the square root of the distance from onset $\sqrt{\mu - \mu_{dp}}$. Because the motion is slow, it is said to *drift*. The motion is along the circle, the *group orbit* of states related by rotation. The variable ζ can be considered to break the symmetry and determine a direction of motion. At the bifurcation, there are two zero eigenvalues: the marginal eigenvector already mentioned above pointing in the θ direction and the new eigenvector in the ζ direction. At the bifurcation point, the Jacobian contains a Jordan block $\begin{bmatrix} 0 & 1 \\ 0 & 0 \end{bmatrix}$ corresponding to the marginal and the drift pitchfork eigenvectors.

In terms of functions $W(\rho,\theta)$, W is even in θ about some point θ_0. The marginal eigenvector $\partial W/\partial\theta$ is therefore odd about θ_0. A bifurcation occurs when the real part of another eigenvalue crosses zero. The corresponding eigenvector (or pair of eigenvectors in the case of a complex eigenvalue) must be either even or odd about θ_0, as was shown in the previous section on reflection symmetry. If the eigenvalue is real and the eigenvector is odd, then a drift pitchfork occurs. From this, it can be seen that drift pitchforks are quite common in situations with $O(2)$ symmetry. Figure 9 shows a bifurcation diagram and solution profiles for a set of reaction-diffusion equations on an interval with $O(2)$ symmetry.

2.4 $O(2)$ and $SO(2)$

We now briefly contrast $O(2)$ and $SO(2)$. The group $SO(2)$ omits the reflection κ. $SO(2)$ symmetry leads to the same equation (46) as in the $O(2)$ case, but, because (44a) and (44b) are not required to be equal, the function $\tilde{f}$ can be complex. Allowing complex coefficients, the normal form (47) becomes

$$\frac{dz}{dt} = (\mu + i\omega - (\alpha + i\beta)|z|^2)z \tag{63}$$

whose polar form is:

$$\frac{d\,(re^{i\theta})}{dt} = \left(\frac{dr}{dt} + ri\frac{d\theta}{dt}\right)e^{i\theta} = ((\mu - \alpha r^2) + i(\omega + \beta r^2))\; r\; e^{i\theta} \tag{64}$$

$$\frac{dr}{dt} = (\mu - \alpha r^2)\, r \tag{65a}$$

$$\frac{d\theta}{dt} = \omega + \beta r^2 \tag{65b}$$

Thus, contrary to the case of $O(2)$, there is usually motion along the θ direction.

We illustrate the difference between $O(2)$ and $SO(2)$ with the example of Taylor-Couette flow, the flow between differentially rotating concentric cylinders, whose common axis will be assumed to be oriented in the vertical direction for concreteness. See figure 10. Experimentally, long cylinders are used, and theoretical analyses assume translational symmetry in the axial direction, which turns out to be a valid approximation away from the regions very near the top and bottom endplates. In an incompressible fluid without free boundaries, gravity is subsumed in the pressure and hence the axial direction is also reflection-symmetric. Thus, there is $O(2)$ symmetry in the axial direction. The azimuthal direction is rotationally symmetric. However, the imposed rotation of the cylinders serves to differentiate clockwise from counter-clockwise rotation, and hence the azimuthal direction has only $SO(2)$ symmetry.

When the two cylinders rotate in the same direction, the first transition to occur breaks the axial ($O(2)$) symmetry and leads to Taylor-vortices, shown on the left in figure 10. These are steady states which resemble tori stacked vertically along the axis of the cylinders. In the infinite-length context, a pair of these vortices define an axially periodic domain and the phase parametrizes a circle of steady states. The azimuthal symmetry is retained.

In contrast, when the ratio between the cylinders' rotation rates is sufficiently negative, the first transition is to spirals, shown on the right in figure 10, which break the azimuthal ($SO(2)$) symmetry as well as

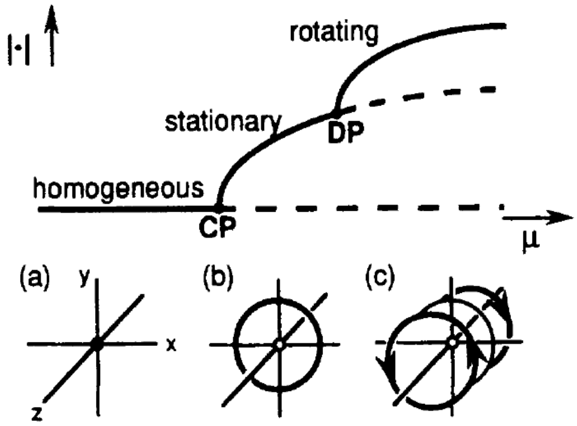

Figure 8: Above: schematic bifurcation diagram showing circle pitchfork (CP) followed by drift pitchfork (DP). Below: schematic phase portraits in (r, θ, ζ) coordinates.

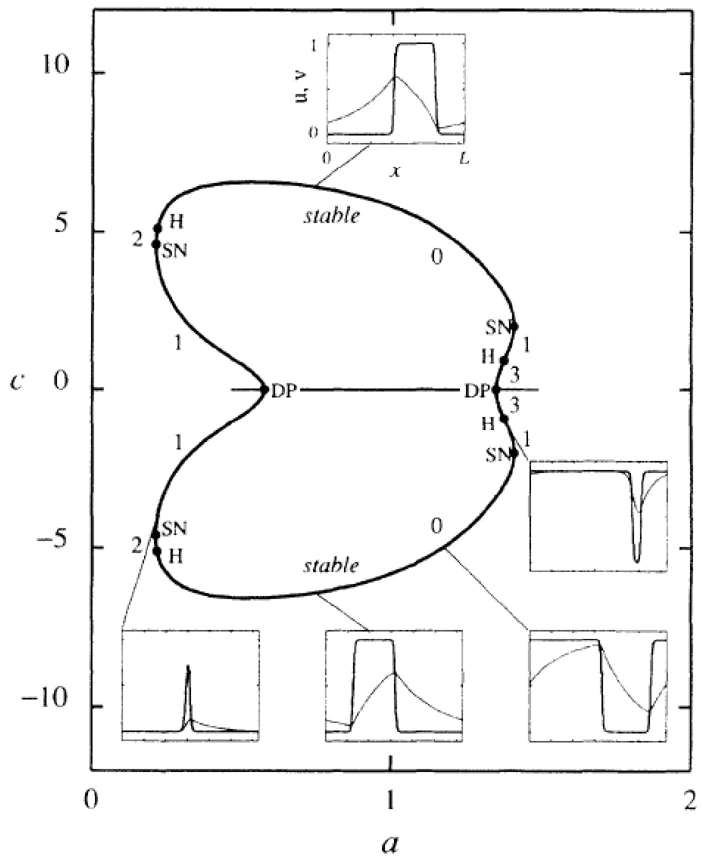

Figure 9: Bifurcation diagram and profiles in u, v for reaction-diffusion system with $O(2)$ symmetry in the x direction. Bifurcation parameter is a and wavespeed is c. The profiles for wavespeeds c and $-c$ are related by reflection in x. From Kness, Tuckerman & Barkley, *Phys. Rev. A* **46**, 5054 (1992).

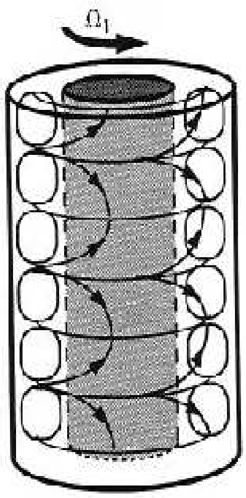

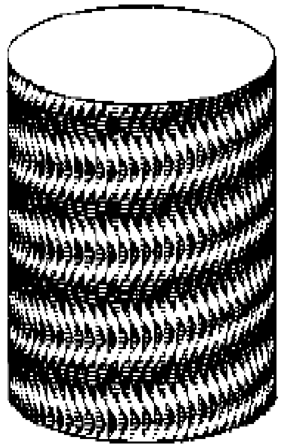

Figure 10: Left: axisymmetric Taylor vortices (reproduced from Tagg, *Nonlinear Science Today* **4**, 1 (1994)). Right: spiral Taylor vortices (reproduced from Antonijoan et al., *Phys. Fluids* **10**, 829 (1995)).

the axial symmetry. These spirals have a well-defined rotation rate in the azimuthal direction. However, because of the axial reflection-symmetry, spirals of two varieties exist, of opposite chirality and direction of motion in the axial direction.

2.5 Hopf bifurcation and $O(2)$ symmetry

The normal form (47) is inadequate for describing many phenomena which occur in an $O(2)$ symmetric configuration, such as Hopf bifurcation and more complicated spatial structures. This is a consequence of the inadequacy of (37), which is only one of many representations of the group $O(2)$. In particular, the two-dimensional normal form (47) cannot describe a Hopf bifurcation which breaks $O(2)$ symmetry. Such a Hopf bifurcation involves a four-dimensional eigenspace. The coefficients of $\cos(\theta)$ and $\sin(\theta)$ obey identical equations, leading to a block diagonal Jacobian. Thus, these coefficients must each be coupled to another variable in order for the Jacobian to have complex eigenvalues.

Having justified the need for a four-dimensional normal form, we consider a field u as represented by

$$u(\theta, t) = \Big[(z_+(t) + z_-(t))e^{i\theta} + (\bar{z}_+(t) + \bar{z}_-(t))e^{-i\theta}\Big] \tag{66}$$

where z_+ is the complex amplitude (representing the amplitude and phase) of left-going traveling waves and z_- is that of right-going traveling waves. At linear order, the evolution of $z_\pm(t)$ is described by

$$\frac{d}{dt}\begin{pmatrix} z_+ \\ z_- \end{pmatrix} = \begin{pmatrix} i\omega z_+ \\ -i\omega z_- \end{pmatrix} \tag{67}$$

so that the linear evolution is

$$u(\theta, t) = z_+(0)e^{i(\theta+\omega t)} + z_-(0)e^{i(\theta-\omega t)} + \bar{z}_+(0)e^{-i(\theta+\omega t)} + \bar{z}_-(0)e^{-i(\theta-\omega t)} \tag{68}$$

with $z_\pm(0)$ arbitrary initial amplitudes.

The addition of nonlinear terms compatible with the $O(2)$ symmetry greatly restricts the possible equilibria. The appropriate representation of $O(2)$ on four-dimensional vectors (z_+, z_-) is:

$$S_{\theta_0}(z_+, z_-) = (e^{i\theta_0} z_+, e^{i\theta_0} z_-) \tag{69a}$$
$$\kappa(z_+, z_-) = (\bar{z}_-, \bar{z}_+) \tag{69b}$$

The mathematics of the derivation of the normal form are also more complicated than in the case of a steady bifurcation. Without justification, we give the simplest cubic order equivariant system of evolution equations:

$$\frac{d}{dt}\begin{pmatrix} z_+ \\ z_- \end{pmatrix} = \begin{pmatrix} \left[\mu + i\omega + a|z_-|^2 + b(|z_+|^2 + |z_-|^2)\right] z_+ \\ \left[\mu - i\omega + \bar{a}|z_+|^2 + \bar{b}(|z_+|^2 + |z_-|^2)\right] z_- \end{pmatrix} \tag{70}$$

Defining $z_\pm = r_\pm e^{i\phi_\pm}$ and $A^2 = r_+^2 + r_-^2$, from (70) we derive:

$$\frac{dr_\pm}{dt} = (\mu + a_r r_\mp^2 + b_r(r_+^2 + r_-^2))r_\pm \tag{71a}$$
$$\frac{d\phi_\pm}{dt} = \pm(\omega + a_i r_\mp^2 + b_i(r_+^2 + r_-^2)) \tag{71b}$$

Note that the equations (70) are independent of the phases $\phi_\pm$.
The solutions for which $dr_\pm/dt = 0$ are:

$$\text{the origin}: \quad r_+ = 0,\ r_- = 0 \tag{72a}$$
$$\text{the left traveling waves}: \quad r_+ = \sqrt{-\mu/b_r},\ r_- = 0, \quad \dot{\phi}_+ = \omega - \mu b_i/b_r \tag{72b}$$
$$\text{the right traveling waves}: \quad r_+ = 0,\ r_- = \sqrt{-\mu/b_r}, \quad \dot{\phi}_- = -(\omega - \mu b_i/b_r) \tag{72c}$$
$$\text{the standing waves}: \quad r_+ = r_- = \sqrt{-\mu/(a_r + 2b_r)}, \quad \dot{\phi}_\pm = \pm(\omega - \mu(a_i + 2b_i)/(a_r + 2b_r)) \tag{72d}$$

Standing and travelling waves are illustrated for a simulation of Rayleigh-Bénard convection in a cylindrical container in figures 11 and 12. Standing and travelling waves are illustrated for 2D simulations of thermosolutal convection in figure 13.

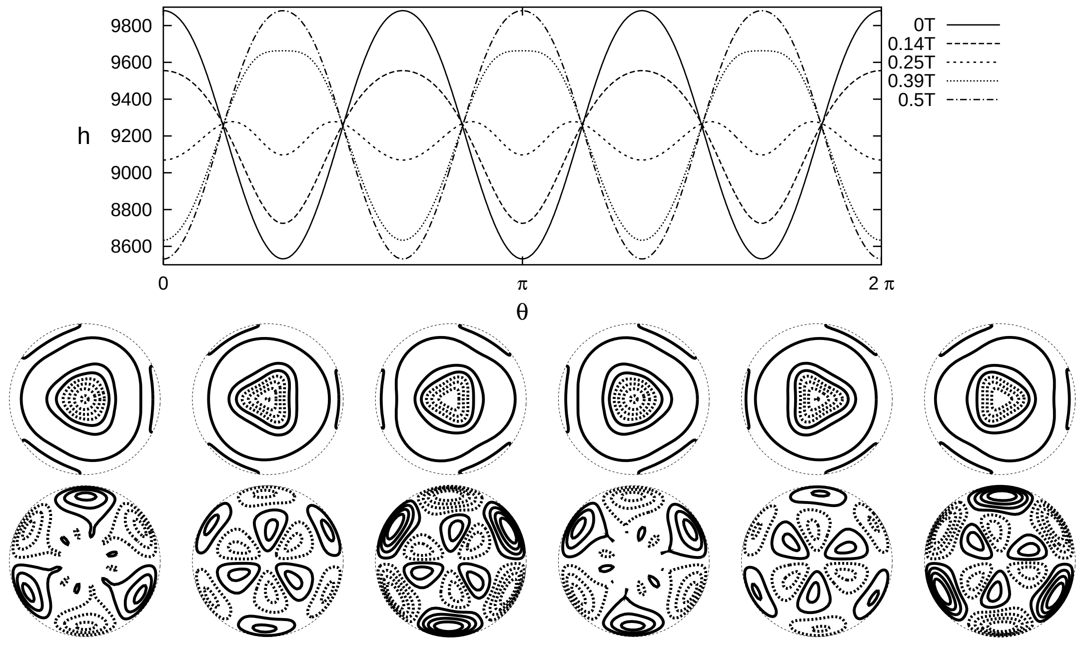

Figure 11: Standing waves in Rayleigh-Bénard convection in a cylinder with $\Gamma = R/H = 1.47$ and $Pr = 1$ at at $Ra = 26\,000$. Top row: temperature versus θ at $(r, z) = (0.7, 0.3)$ at five successive times during one oscillation period T. Middle and bottom rows: contours of temperature (middle) and of azimuthal velocity (bottom) on the midplane at $t = 0$, $T/6$, $2T/6$, $3T/6$, $4T/6$, $5T/6$. From Borońska & Tuckerman, J. Fluid Mech. **559**, 279 (2006).

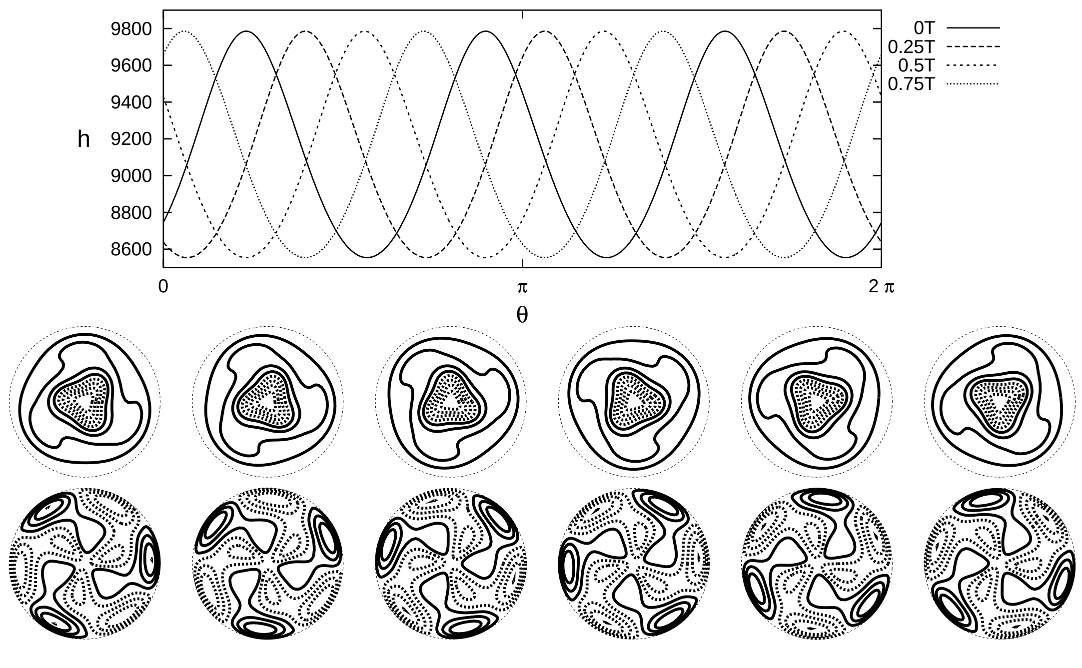

Figure 12: Counterclockwise travelling wave in Rayleigh-Bénard convection in a cylinder with $\Gamma = R/H = 1.47$ and $Pr = 1$ at $Ra = 26\,000$. Top row: temperature versus angle θ for $(r, z) = (0.7, 0.3)$, at four different instants during one oscillation period T. Middle and bottom rows: contours of temperature (middle) and of azimuthal velocity (bottom) on the midplane at $t = 0$, $T/6$, $2T/6$, $3T/6$, $4T/6$, $5T/6$. From Borońska & Tuckerman, J. Fluid Mech. **559**, 279 (2006).

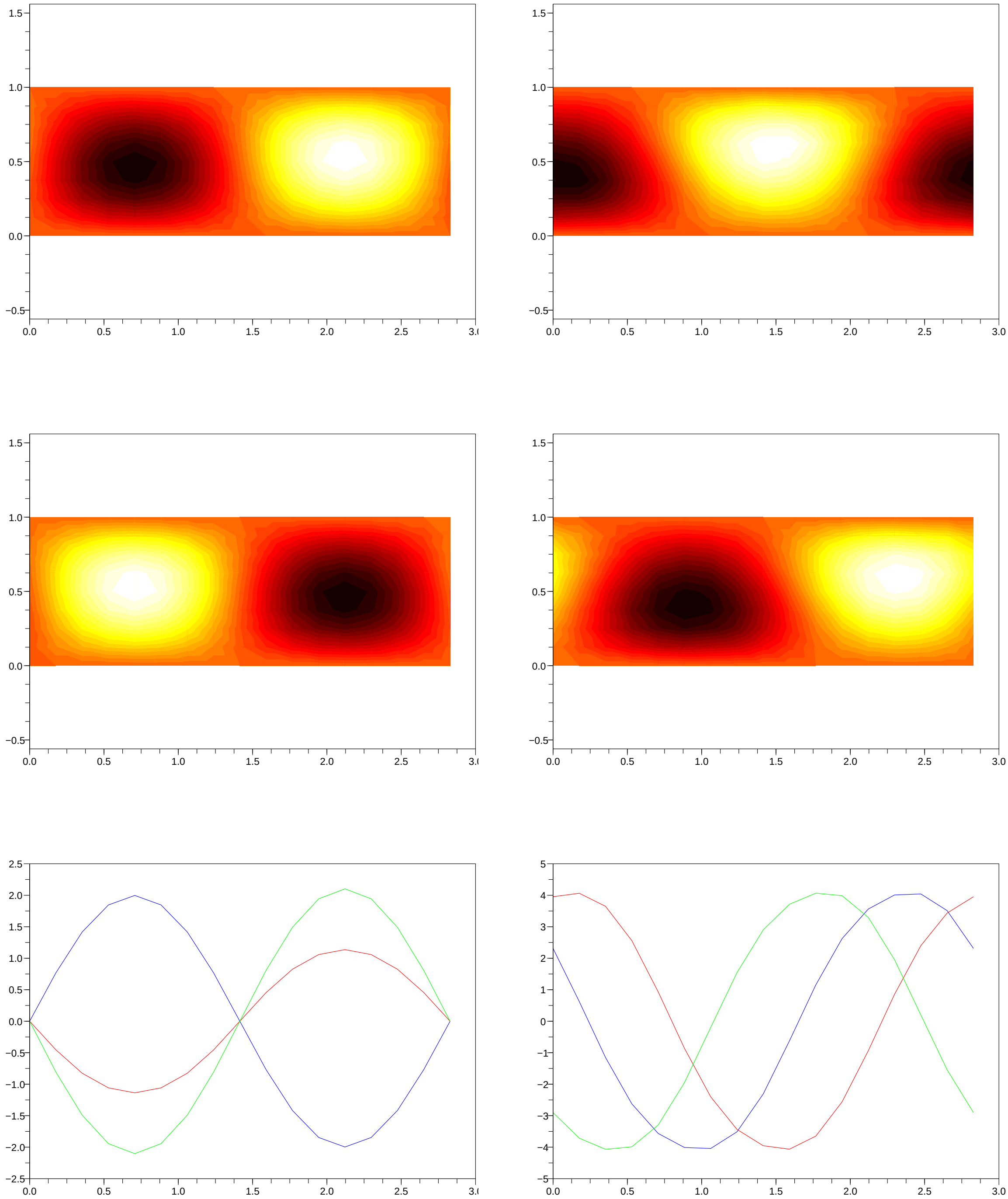

Figure 13: Simulation of 2D thermosolutal convection with horizontally periodic and vertical free-slip boundary conditions. Parameters are $S = -0.1$, $L = 0.1$, $Pr = 10$, and $r \equiv Ra/Ra_c = 1.3$. Above: temperature field at two successive times. Below: wave profiles at mid-height at successive times. Left: standing waves. Right: travelling waves.

According to the signs and magnitudes of a and b, the standing waves and traveling waves branch in the same or the opposite directions in μ. If $b_r < 0$ (> 0), then the travelling waves exist for $\mu > 0$ (< 0) If $a_r + 2b_r < 0$ (> 0), then the standing waves exist for $\mu > 0$ (< 0). The lines $b_r = 0$ and $a_r + 2b_r = 0$ thus divide the (a_r, b_r) plane into four sections, as shown in figure 15.

The stability of these states is calculated as follows. At the origin, since angles are not defined, we must write the Jacobian in its Cartesian representation. as we did in equation (51) concerning the circle pitchfork. We will not do this here and just state that at the origin, the Jacobian is μ times the identity and hence has four eigenvalues which change sign at μ, along with a four-dimensional eigenspace.

For the non-zero states, we can write the Jacobian in the polar $(r_+, r_-, \phi_+, \phi_-)$ coordinates:

$$\begin{pmatrix} \mu + a_r r_-^2 + b_r(r_+^2 + r_-^2) + 2b_r r_+^2 & 2(a_r + b_r)r_- r_+ & 0 & 0 \\ 2(a_r + b_r)r_- r_+ & \mu + a_r r_+^2 + b_r(r_+^2 + r_-^2) + 2b_r r_-^2 & 0 & 0 \\ 2b_i r_+ & 2(a_i + b_i)r_- & 0 & 0 \\ -2(a_i + b_i)r_+ & -2b_i r_+ & 0 & 0 \end{pmatrix} \tag{73}$$

Since (73) is block lower-triangular, its eigenvalues and eigenvectors are those of its diagonal blocks, as shown by:

$$\begin{pmatrix} A & 0 \\ C & D \end{pmatrix} \begin{pmatrix} X \\ Y \end{pmatrix} = \lambda \begin{pmatrix} X \\ Y \end{pmatrix} \tag{74}$$

$$\left. \begin{array}{r} AX = \lambda X \\ CX + DY = \lambda Y \end{array} \right\} \Longrightarrow \left\{ \begin{array}{l} X = 0 \\ (\lambda, Y) \text{ is an eigenpair of } D \end{array} \right\} \text{ or } \left\{ \begin{array}{l} (\lambda, X) \text{ is an eigenpair of } A \\ Y = (\lambda I - D)^{-1} CX \end{array} \right\} \tag{75}$$

(In (75), A, B, C, D, X, Y are unrelated to the notation used for the Hopf-$O(2)$ problem.) The directions $\phi_\pm$ are thus neutral directions.

The eigenvalues of the $r_\pm$ direction are obtained via the formula for a general 2×2 matrix $\begin{pmatrix} a & b \\ c & d \end{pmatrix}$:

$$\lambda_\pm = \frac{a+d}{2} \pm \sqrt{\left(\frac{a-d}{2}\right)^2 + bc} \tag{76}$$

(Again, in (76), a, b, c, d are unrelated to the notation used for the Hopf-$O(2)$ problem.) Substituting the elements of (73) and the solutions (72) into (76) leads to

$$\begin{array}{lll} \text{the origin :} & \mu \text{ along } r_+ & \mu \text{ along } r_- \\ \text{the left traveling waves :} & -2\mu \text{ along } r_+ & -a_r\mu/b_r \text{ along } r_- \\ \text{the right traveling waves :} & -2\mu \text{ along } r_- & -a_r\mu/b_r \text{ along } r_+ \\ \text{the standing waves :} & -2\mu \text{ along } (r_+, r_-) & 2a_r\mu/(a_r + 2b_r) \text{ perpendicular to } (r_+, r_-) \end{array} \tag{77}$$

If $b_r < 0$, then the travelling waves exist for $\mu > 0$, as shown in (72). Since $-2\mu < 0$, they are stable if and only if $a_r/b_r > 0$, i.e. in the lower left quadrant of the (a_r, b_r) plane, as shown in figure 15. If $b_r > 0$, then the travelling waves exist for $\mu < 0$, so $-2\mu > 0$ and they are not stable. Similarly, if $a_r + 2b_r < 0$, then the standing waves exist for $\mu > 0$ and they are stable if $a_r > 0$, i.e. in the upper-left wedge of the (a_r, b_r) plane. If $a_r + 2b_r > 0$, then the standing waves exist for $\mu < 0$ and so $-2\mu > 0$ and they are not stable.

Some general conclusions are that either the standing waves or the traveling waves are stable, or neither are stable. If one solution is stable, it is that which has the largest amplitude $\sqrt{r_+^2 + r_-^2}$. If neither are

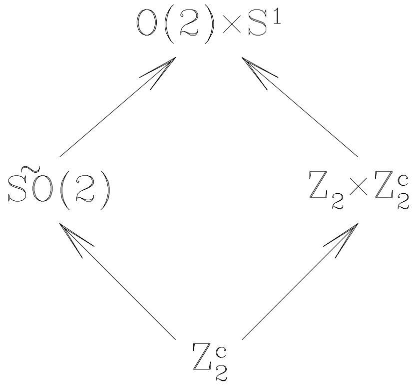

Figure 14: Lattice of isotropy subgroups for $O(2) \times S^1$. Travelling waves have the isotropy subgroup $\tilde{SO}(2)$, standing waves have the isotropy subgroup $Z_2 \times Z_2^c$.

stable, then $r_\pm \to \infty$ for some choices of initial conditions or μ-values, unless higher order terms are added to (71a) or (70). This is shown in figures 15 and 16.

To write down the symmetries of the solutions, we must introduce another transformation, namely that of translation in time:

$$T_{t_0} u(t) \equiv u(t + t_0) \tag{78}$$

The group of all the translations in time S_{t_0} is called S^1. The original homogeneous stationary state, before bifurcation to waves, has the full space-time symmetry group $O(2) \times S^1$. A travelling wave solution has the space-time symmetry

$$(T_{t_0} S_{\omega t_0} u)(\theta, t) \equiv u(\theta + \omega t_0, t + t_0) = u(\theta, t) \tag{79}$$

for any t_0. This set of space-time symmetries, parametrized by t_0, forms a group isomorphic to $SO(2)$, which is called $\widetilde{SO}(2)$. The subgroup of transformations leaving a particular solution invariant is called its *isotropy subgroup*; the isotropy subgroup of a travelling wave solution is $\widetilde{SO}(2)$. Standing waves have an ordinary spatial reflection symmetry in θ:

$$(\kappa u)(\theta, t) \equiv u(-\theta) = u(\theta, t) \tag{80}$$

(For simplicity, we have taken the axis of reflection, which does not move, to be at $\theta = 0$.) Standing waves also have the space-time reflection symmetry:

$$(T_{\pi/\omega} S_\pi u)(\theta, t) \equiv u(\theta + \pi, t + \pi/\omega) = u(\theta, t) \tag{81}$$

The transformation in (81) is called Z_2^c and is a special case of that in (79). The group of transformations leaving a standing wave solution invariant, i.e. its isotropy subgroup, is called $Z_2 \times Z_2^c$. We can arrange the original symmetry group and the isotropy subgroups in a diagram called the *lattice of isotropy subgroups*, as shown in figure 14.

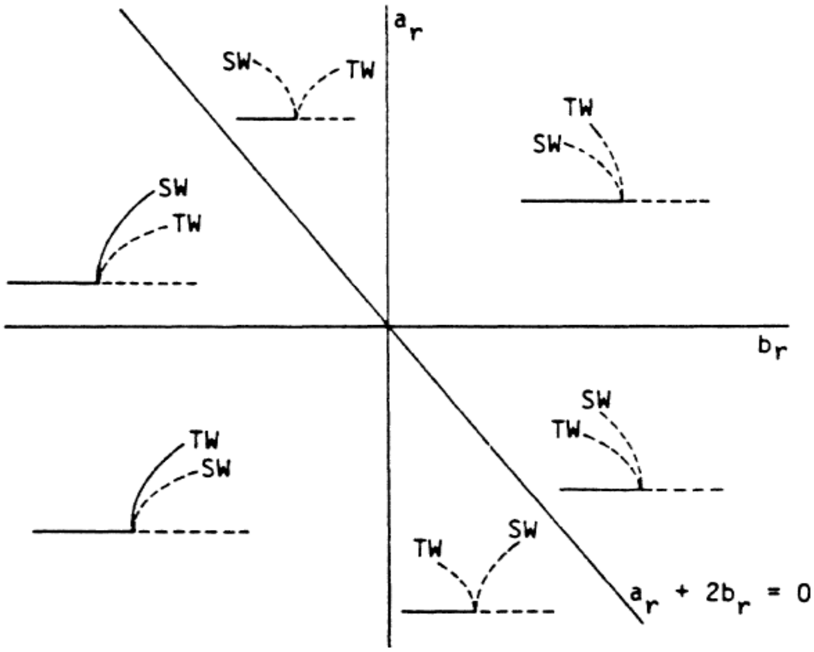

Figure 15: Stability and branching direction of standing waves (SW) and travelling waves (TW) in the parameter plane of the nonlinear coefficients (a_r, b_r). From Knobloch, Phys. Rev. A **34**, 1538 (1986).

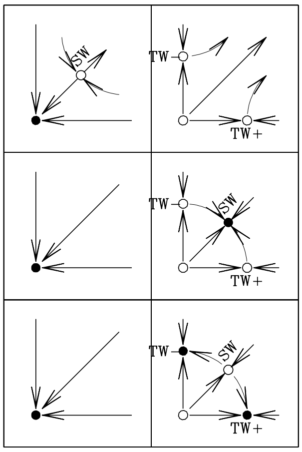

Figure 16: Phase diagrams for Hopf bifurcation with $O(2)$ symmetry when $b_r < 0$. Each diagram shows the (r_+, r_-) plane. Left diagrams: $\mu < 0$. Right diagrams: $\mu > 0$. Top row: $-2b_r < a_r$. Middle row: $0 < a_r < -2b_r$. Bottom row: $a_r < 0$.

2.6 Steady-state mode interactions

Let us return to a description in terms of a function w of (ρ, θ) where θ is a direction with reflection and translation symmetry. The instability of a state which is homogeneous (featureless) in θ will be governed by a system of linear partial differential equations which is also homogeneous in θ. The solutions to such equations are necessarily exponential or trigonometric in θ. If we wish to study pattern formation, i.e. a repeating motif, then we restrict further to a trigonometric dependence. Definition (41) included only one spatial wavenumber. Let us generalize (41) to include two wavenumbers, m and n, for the θ dependence, in order to describe situations in these two spatial structures compete and interact. We write:

$$w(\rho,\theta) = \frac{1}{2}\left(z_m(\rho)e^{im\theta} + z_n(\rho)e^{in\theta} + \bar{z}_m(\rho)e^{-im\theta} + \bar{z}_n(\rho)e^{-in\theta}\right) \tag{82}$$

Reflection in θ and rotation (translation) θ should have the effect:

$$\begin{aligned}(S_{\theta_0}w)(\rho,\theta) = w(\rho,\theta+\theta_0) &= \frac{1}{2}\Big(z_m(\rho)e^{im(\theta+\theta_0)} + z_n(\rho)e^{in(\theta+\theta_0)} \\ &+ \bar{z}_m(\rho)e^{-im(\theta+\theta_0)} + \bar{z}_n(\rho)e^{-in(\theta+\theta_0)}\Big) \qquad \text{(83a)}\\ (\kappa w)(\rho,\theta) = w(\rho,-\theta) &= \frac{1}{2}\Big(z_m(\rho)e^{-im\theta} + z_n(\rho)e^{-in\theta} \\ &+ \bar{z}_m(\rho)e^{im\theta} + \bar{z}_n(\rho)e^{in\theta}\Big) \qquad \text{(83b)}\end{aligned}$$

This motivates us to prescribe the action of S_{θ_0} on (z_m, z_n):

$$\begin{aligned} S_{\theta_0}(z_m,z_n) &= (e^{im\theta_0}\, z_m, e^{in\theta_0}\, z_n) \qquad \text{(84a)}\\ \kappa(z_m,z_n) &= (\bar{z}_m, \bar{z}_n) \qquad \text{(84b)}\end{aligned}$$

We now seek the general form of functions $f(z_m, z_n)$ which are equivariant with respect to (84). We consider monomials

$$f(z_m,z_n) = \begin{pmatrix} f_m \\ f_n \end{pmatrix}(z_m,z_n) = \begin{pmatrix} f_{mpqrs} z_m^p z_n^q \bar{z}_m^r \bar{z}_n^s \\ f_{npqrs} z_m^p z_n^q \bar{z}_m^r \bar{z}_n^s \end{pmatrix} \tag{85}$$

As in the single-wavenumber case, equivariance with respect to κ leads to the requirement that the coefficients in (85) be real. Equivariance with respect to S_θ leads to

$$\begin{aligned} S_\theta f(z_m,z_n) &= \begin{pmatrix} e^{im\theta} f_{mpqrs} z_m^p z_n^q \bar{z}_m^r \bar{z}_n^s \\ e^{in\theta} f_{npqrs} z_m^p z_n^q \bar{z}_m^r \bar{z}_n^s \end{pmatrix} \qquad \text{(86a)}\\ f S_\theta(z_m,z_n) &= \begin{pmatrix} f_{mpqrs}(e^{im\theta}z_m)^p(e^{in\theta}z_n)^q(e^{-im\theta}\bar{z}_m)^r(e^{-in\theta}\bar{z}_n)^s \\ f_{npqrs}(e^{im\theta}z_m)^p(e^{in\theta}z_n)^q(e^{-im\theta}\bar{z}_m)^r(e^{-in\theta}\bar{z}_n)^s \end{pmatrix} \qquad \text{(86b)}\end{aligned}$$

This leads to the requirements that:

$$\begin{aligned} f_{mpqrs} = 0 \ \text{ or } \ m = mp + nq - mr - ns \qquad \text{(87a)}\\ f_{npqrs} = 0 \ \text{ or } \ n = mp + nq - mr - ns \qquad \text{(87b)}\end{aligned}$$

Using (87), it is possible to ascertain that a basis for the invariants is:

$$|z_m|^2, |z_n|^2, \ \text{ and } \ \Delta \equiv z_m^n \bar{z}_n^m + \bar{z}_m^n z_n^m \tag{88}$$

i.e. that all invariants are products and sums of these three, and that a basis for the equivariants is:

$$\begin{pmatrix} z_m \\ 0 \end{pmatrix}, \begin{pmatrix} 0 \\ z_n \end{pmatrix}, \begin{pmatrix} \bar{z}_m^{n-1} z_n^m \\ 0 \end{pmatrix}, \begin{pmatrix} 0 \\ z_m^n \bar{z}_n^{m-1} \end{pmatrix} \tag{89}$$

meaning that all equivariants are sums of these four, with coefficients which are invariants. Thus, the most general equivariant evolution equation is of the form

$$\frac{d}{dt}\begin{pmatrix} z_m \\ z_n \end{pmatrix} = a\begin{pmatrix} z_m \\ 0 \end{pmatrix} + b\begin{pmatrix} 0 \\ z_n \end{pmatrix} + c\begin{pmatrix} \bar{z}_m^{n-1} z_n^m \\ 0 \end{pmatrix} + d\begin{pmatrix} 0 \\ z_m^n \bar{z}_n^{m-1} \end{pmatrix} \tag{90}$$

where a, b, c, d are functions of $(|z_m|^2, |z_n|^2, \Delta)$.

Let us now consider (90) truncated to cubic order. If $m + n - 1 > 3$, then neither the last invariant nor the last two equivariants contribute at this order, and the most general equivariant is:

$$(a_0 + a_m|z_m|^2 + a_n|z_n|^2)\begin{pmatrix} z_m \\ 0 \end{pmatrix} + (b_0 + b_m|z_m|^2 + b_n|z_n|^2)\begin{pmatrix} 0 \\ z_n \end{pmatrix} \tag{91}$$

That is, the most general set of evolution equations in the case that $m + n - 1 > 3$ is independent to cubic order of the values of m and n and is:

$$\frac{dz_m}{dt} = (a_0 + a_m|z_m|^2 + a_n|z_n|^2)z_m \tag{92a}$$

$$\frac{dz_n}{dt} = (b_0 + b_m|z_m|^2 + b_n|z_n|^2)z_n \tag{92b}$$

Since the coefficients a, b are real, the phases play no role and we may replace the complex z_m, z_n by real values x_m, x_n. The equations are then just those that apply to the case of rectangular symmetry, $Z_2 \times Z_2$. Let us calculate the steady states of (92). We have

$$x_m = 0 \quad \text{or} \quad a_0 + a_m x_m^2 + a_n x_n^2 = 0 \quad \text{and} \tag{93a}$$

$$x_n = 0 \quad \text{or} \quad b_0 + b_m x_m^2 + b_n x_n^2 = 0 \tag{93b}$$

We may plot the conditions in equations (93) in a two-dimensional plane (x_m, x_n). The conditions on the left are the two perpendicular axes, while those on the right are equations for ellipses or hyperbolas, depending on the signs of coefficients a, b. The steady states are the intersections of conditions (93a) with conditions (93b), the existence of which depend on the values of coefficients a, b. An example of this graphical construction is shown in figure 17, as a function of bifurcation parameter μ for coefficients $a_0 = \mu$, $b_0 = \mu - 1$, $a_m = b_n = -1$, $a_n = b_m = -2$.

$$\text{the origin}: \quad x_m = 0,\ x_n = 0 \tag{94a}$$

$$\text{the pure } m \text{ modes}: \quad x_m^2 = -a_0/a_m,\ x_n = 0 \tag{94b}$$

$$\text{the pure } n \text{ modes}: \quad x_m = 0,\ x_n^2 = -b_0/b_n \tag{94c}$$

$$\text{the mixed modes}: \quad x_m^2 = \frac{a_0 b_n - b_0 a_n}{b_m a_n - a_m b_n},\quad x_n^2 = \frac{a_0 b_m - b_0 a_m}{-(b_m a_n - a_m b_n)} \tag{94d}$$

The lattice of isotropy subgroups is shown in figure 19.

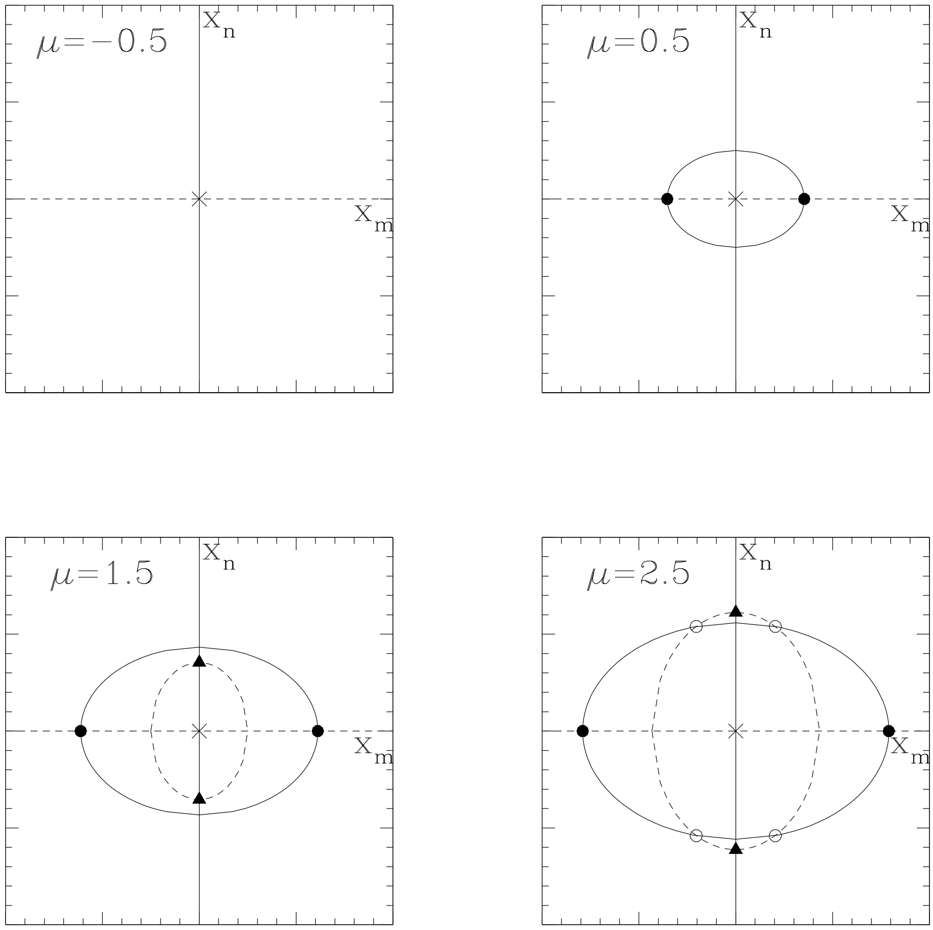

Figure 17: Graphical construction for steady solutions (x_m, x_n). Solid curves are solutions to conditions (93a), dashed curves are solutions to conditions (93b). Steady states are intersections of the two types of curves, where one of conditions (93a) and one of conditions (93b) are simultaneously satisfied. Solid dots are pure m modes, solid triangles are pure n modes, and open circles are mixed modes. For the coefficient values $a_0 = \mu$, $b_0 = \mu - 1$, $a_m = b_n = -1$, $a_n = b_m = -2$ used here, the pure m mode appears at $\mu = 0$, the pure n mode at $\mu = 1$, and the mixed modes at $\mu = 2$.

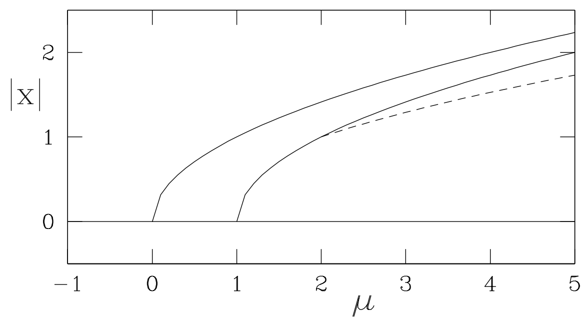

Figure 18: Bifurcation diagram for (x_m, x_n). $|x| \equiv \sqrt{(x_m^2 + x_n^2)}$ as a function of μ. Solid curves: pure modes. Dashed curve: mixed mode.

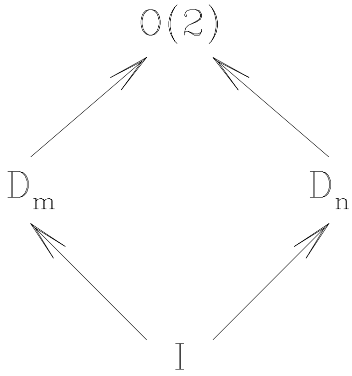

Figure 19: Lattice of isotropy subgroups for (m, n) mode interaction.

2.7 Quotient groups

We return to the finite group D_4 which describes the symmetries of a square and will illustrate some basic group-theoretic ideas. D_4 has two *generators*, which we choose to be rotation by angle $\pi/2$ and reflection in y, as in equations (37), meaning that all elements of the group can be generated by products of these two elements. In this section, we denote the identity by e, rotation by $\pi/2$ by ρ and reflection in y by κ. The group table for D_4 is shown below in tabular form. A color version is shown in figure 20.

e	e	ρ	ρ^2	ρ^3	κ	$\kappa\rho$	$\kappa\rho^2$	$\kappa\rho^3$
e	e	ρ	ρ^2	ρ^3	κ	$\kappa\rho$	$\kappa\rho^2$	$\kappa\rho^3$
ρ	ρ	ρ^2	ρ^3	e	$\kappa\rho$	$\kappa\rho^2$	$\kappa\rho^3$	κ
ρ^2	ρ^2	ρ^3	e	ρ	$\kappa\rho^2$	$\kappa\rho^3$	κ	$\kappa\rho$
ρ^3	ρ^3	e	ρ	ρ^2	$\kappa\rho^3$	κ	$\kappa\rho$	$\kappa\rho^2$
κ	κ	$\kappa\rho^3$	$\kappa\rho^2$	$\kappa\rho$	e	ρ^3	ρ^2	ρ
$\kappa\rho$	$\kappa\rho$	κ	$\kappa\rho^3$	$\kappa\rho^2$	ρ	e	ρ^3	ρ^2
$\kappa\rho^2$	$\kappa\rho^2$	$\kappa\rho$	κ	$\kappa\rho^3$	ρ^2	ρ	e	ρ^3
$\kappa\rho^3$	$\kappa\rho^3$	$\kappa\rho^2$	$\kappa\rho$	κ	ρ^3	ρ^2	ρ	e

(95)

As is the case for all group tables, each element of D_4 appears exactly once in each row and in each column. D_4 has a number of *subgroups*, namely:

$$\text{One one-element subgroup:} \quad \{e\} \tag{96a}$$

$$\text{Five two-element subgroups:} \quad \{e, \rho^2\}, \quad \{e, \kappa\}, \quad \{e, \kappa\rho\}, \quad \{e, \kappa\rho^2\}, \quad \{e, \kappa\rho^3\} \tag{96b}$$

$$\text{Two four-element subgroups:} \quad \{e, \rho, \rho^2, \rho^3\}, \quad \{e, \rho^2, \kappa, \kappa\rho^2\} \tag{96c}$$

The number of elements in each subgroup is a divisor of the number of elements of D_4. The two four-element subgroups are of different kinds. The subgroup $\{e, \rho, \rho^2, \rho^3\}$ is *isomorphic* to (has the structure of) Z_4, while the subgroup $\{e, \rho^2, \kappa, \kappa\rho^2\}$ is isomorphic to $Z_2 \times Z_2$, as can be seen from the fact that each element is its own inverse.

The table shows clearly that D_4 has a kind of large-scale structure. The single lines divide the group into two sets, one consisting of the rotations (which resembles the identity), and the other of the reflections (which resembles a reflection). The large-scale structure is that of Z_2. Formally, the subroup $N \equiv$

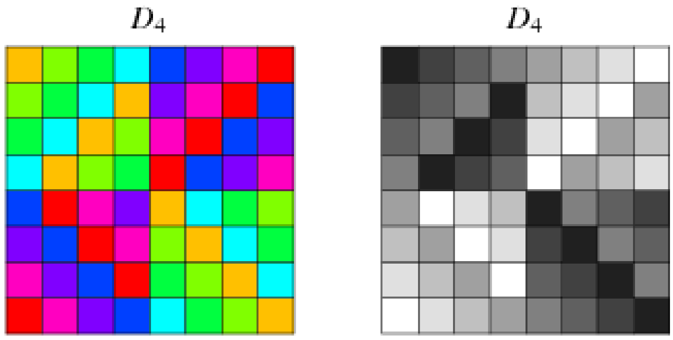

Figure 20: Pictorial version of table of group D_4. From *Mathworld*, by Eric Weisstein, Wolfram Research.

$\{e, \rho, \rho^2, \rho^3\}$ of rotations is a *normal* subgroup of $\Gamma \equiv D_4$, meaning that $gng^{-1} \in N$ for all elements $g \in \Gamma$, $n \in N$. When a group N is normal, one can form the *quotient group* Γ/N. In this case, Γ/N is isomorphic to Z_2, and this is the large-scale structure that we see in the D_4 table. The number of elements or *order* of Γ/N is the order of Γ divided by the order of N. We will not go more deeply into group theory at this time.

3 Exercises

1. Consider the symmetry group consisting of the identity and the reflection $(\kappa u)(x) \equiv u(-x)$. Note that κ acts on a function to create another function. Which of the following terms is equivariant with respect to this symmetry group? (u' is the derivative of u with respect to x.)
a) uu' b) u^2 c) $(u')^2$
Consider for this purpose an operator $\mathcal{F}$ which also transforms functions into other functions. For example in (a), $\mathcal{F}$ acts on a function u to produce another function which is the product of u and its derivative u'. The question is whether κ and $\mathcal{F}$ commute.

2. Draw phase diagrams for the Hopf bifurcation with $O(2)$ symmetry like those in figure 16, but for $b_r > 0$.

3. Write the group table for D_3, the symmetry group of the equilateral triangle. List its subgroups and state which are normal subgroups.

4. Consider the configurations in figure 21: a circle, a rotating circle, an ellipse, and a rotating ellipse. Suppose each picture represents a container of fluid, seen from above, in a Rayleigh-Bénard convection experiment. The temperature gradient points into the page, the lower surface is solid and the upper surface is a free surface. What are the symmetries and the symmetry group for each experiment?

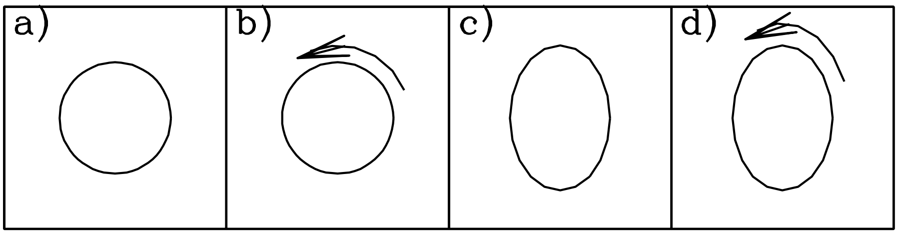

Figure 21: Four configurations. a) Circle. b) Rotating circle. c) Ellipse. d) Rotating ellipse.